J Mater Sci (2010) 45:5309–5317
DOI 10.1007/s10853-010-4576-3

Analysis of growth parameters for hydrothermal synthesis of ZnO nanoparticles through a statistical experimental design method

Shao-Hwa Hu · Yi-Chuan Chen · Chyi-Ching Hwang · Cheng-Hsiung Peng · Dah-Chuan Gong

Received: 15 January 2010 / Accepted: 28 April 2010 / Published online: 14 May 2010

Abstract Nanocrystalline ZnO particles were synthesized from an aqueous solution composed of zinc acetate dihydrate ($Zn(CH_3COO)_2{\cdot}2H_2O$) and urea ($H_2NCONH_2$). A precipitating precursor, basic zinc carbonate ($Zn_5(CO_3)_2(OH)_6$), was first formed by hydrothermally treating the solution at 120 °C for 2–4 h. Nanocrystalline ZnO particles were then obtained by calcining the precursors at 350–650 °C for 0.5–2 h. The synthesis products were characterized using thermogravimetry–differential scanning calorimetry–mass spectrometry, X-ray diffraction, scanning electron microscopy, transmission electron microscopy and photoluminescence techniques. Based on the experimental results, a possible reaction mechanism for the ZnO formation was proposed. The effects of experimental parameters (namely, the hydrothermal treatment time, the calcination time, and the calcination temperature) on the characteristics of the resulting ZnO products (i.e., the crystalline size and the photoluminescence properties) were analyzed by the Taguchi method to attain the optimum synthesis conditions. By using the appropriate parameters derived from this method, we verified that the optimized synthesis provided a yield of ~70% and that the resulting ZnO particles possessed the characteristics of a ~25 nm crystalline size and a satisfactory photoluminescence property.

S.-H. Hu · D.-C. Gong
Department of Industrial and Systems Engineering, College of Electrical Engineering and Computer Science, Chung Yuan Christian University, Chungli, Taoyuan 320, Taiwan, ROC

S.-H. Hu
Chemical Systems Research Division, Chung Shan Institute of Science and Technology, Longtan, Taoyuan 325, Taiwan, ROC

Y.-C. Chen (✉) · C.-C. Hwang
Department of Applied Chemistry and Materials Science, Chung Cheng Institute of Technology, NDU, Dasi, Taoyuan 335, Taiwan, ROC
e-mail: yi.juan@msa.hinet.net

C.-H. Peng
Department of Chemical Engineering and Materials Science, Ming Hsin University of Science and Technology, Hsinfeng, Hsinchu 304, Taiwan, ROC

Introduction

Nanostructured zinc oxide (ZnO) is of interest in the optoelectronic, piezoelectric, sensor, biomedical, and electrochemical fields because of its interesting characteristics, such as a direct band gap of 3.37 eV, a large exciton binding energy of 60 meV at room temperature, transparent conductivity, noncentrosymmetric symmetry, biosafety, and biocompatibility properties [1, 2]. Hence, ZnO has attracted a significant amount of attention from researchers.

Two major categories of techniques have been developed for the synthesis of nanostructured ZnO, namely, vapor-phase processes [3, 4] and wet chemical routes [5–9]. In general, the latter have the potential advantage of larger-scale preparations for high-technology applications. A frequently adopted method begins with a solution of a Zn-containing salt in the presence of a precipitant providing OH^- and/or CO_3^{2-} ions to yield a precipitating precursor. This precursor can then be transformed into ZnO particles by a colloidal technique [7] or heat treatment [8–10].

With regard to the hydrothermal synthesis of nanocrystalline ZnO particles using zinc acetate dihydrate and urea as starting materials, the reaction mechanism for ZnO formation and the effects of processing parameters on the product characteristics have not yet been extensively studied. In this work, a precipitating precursor was

prepared in advance by hydrothermally treating an aqueous solution of zinc acetate dihydrate ($Zn(CH_3COO)_2{\cdot}2H_2O$, hereafter termed as $ZnAc_2$) and urea. The precursor was then calcined to form ZnO nanoparticles. Depending on the experimental parameters, such as hydrothermal time, calcination temperature, and calcination time, it was expected that the resulting ZnO would show different grain shape, crystalline size, photoluminescence (PL) properties, and so on.

It has been shown that efficient analyses of product-quality characteristics can be performed using a statistical experimental design method, i.e., the Taguchi method, which is a combination of mathematical and statistical techniques used in an empirical study [10–13]. This method has been adopted to optimize various synthetic processes of nanostructured materials [10–12] due to its potential advantages of experimental efficiency and reproducibility [10–13]. Therefore, the Taguchi method was utilized in this work to identify the optimal conditions and to select the parameters having the greatest influence on the crystallite size and PL properties of the resulting ZnO products.

The objectives of this work were: (1) to examine the formation mechanism of ZnO nanoparticles synthesized by the proposed route; (2) to apply the Taguchi method to evaluate the effects of the experimental parameters on the crystalline size and PL properties of the resulting ZnO products; and (3) to optimize the experimental parameters and perform verification experiments using the optimal conditions.

Experimental

Synthesis and characterizations

Both the starting materials, $ZnAc_2$ and urea ($(NH_2)_2CO$), were of analytical grade and were purchased from WACO Ltd., Japan. The precursor was first prepared by the following hydrothermal route: 0.05 mol of $ZnAc_2$ and 0.1 mol of urea were dissolved in 100 mL of deionized water at room temperature from a clear and homogenous solution. Then, the mixed solution was transferred into a 120-mL Teflon-lined autoclave and securely sealed. The solution contained in the autoclave was heated in an electronic furnace at a temperature of 120 °C for 2–4 h. The reaction was then quenched using cold water. The precursor was collected by centrifugation, washed with absolute alcohol (99.8%), and then dried in a vacuum oven at 25 °C for 2 h. The desired product, ZnO, was obtained by calcining the dried precursors in a muffle furnace at 350–650 °C for 0.5–2 h. The experimental procedure for preparing the ZnO nanoparticles is shown in Fig. 1.

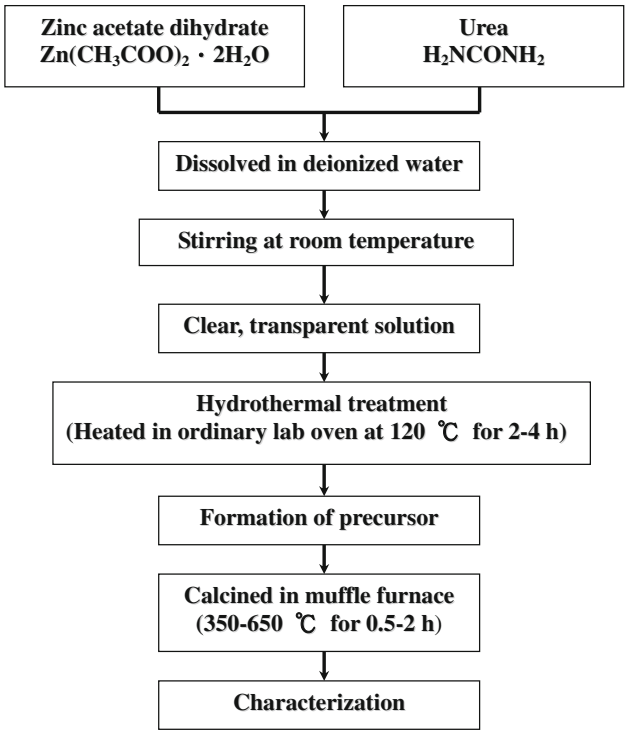

Fig. 1 Experimental procedure for preparing the ZnO nanoparticles

Phase formation was identified by particle X-ray diffraction (XRD), which was performed on a SIEMENS D5000 X-ray diffractometer with Cu $K\alpha_1$ radiation ($\lambda = 0.15406$ nm). In addition, the crystallite size (D) of the calcined particles was calculated by the X-ray line-broadening technique performed on the (1 1 0) diffraction of the ZnO lattice using computer software (Siemens Diffrac AT program V3.10) based on the Scherrer formula [14]:

$$D = \frac{0.9\lambda}{B\cos\theta_B}, \quad (1)$$

where θ_B is the Bragg angle of the diffraction lines, λ is the wavelength of the incident X-ray, and B is the full width at half maximum (FWHM). Fourier-transform infrared spectroscopy (FTIR) measurements were carried out with a Nicolet-870 spectrometer in transmittance mode, where the samples were dispersed in KBr pellets. The morphological features of the samples were observed with scanning electron microscopy (SEM, Hitachi S4800-I) and transmission electron microscopy (TEM, JEOL JEM-2010). The precipitates obtained were simultaneously analyzed by thermogravimetry (TG) and differential scanning calorimetry (DSC), carried out at a heating rate of 10 °C/min in static air (flow rate: 50 cm^3/min) using a thermal analyzer (NETZSCH, Instruments 404). The gas escaping from the TG–DSC cell was analyzed with a mass spectrometer (MS, NETZSCH, QMS Skimmer). PL spectra of the particles were measured at room temperature using an He–Cd laser with a wavelength of 325 nm as the excitation source.

Taguchi design

For our experimental design, we chose to study three parameters that could affect the crystallite size and PL properties of the ZnO nanoparticles: the hydrothermal processing time, the calcination temperature, and the calcination time. In the Taguchi method for optimizing the properties of the ZnO products synthesized through the hydrothermal route, these three experimental parameters were taken as the controlling factors in ZnO synthesis; hydrothermal time was symbolized as A (h), calcination temperature as B (°C), and calcination time as C (h). Each experimental parameter was varied at three levels for study. The three experimental parameters and their corresponding levels are shown in Table 1. A template of the L_9 (3^4) orthogonal array, as given in Liu et al. [10], was selected for study with the Taguchi method, as shown in Table 2. As seen here, there were in total nine experiments needed for this work. Each experiment was repeated three times. Two characteristics of the ZnO products, i.e., the crystallite size (D) and the intensity ratio of UV emission to visible-light emission (R_i), were selected as the quality characteristics and used for response analysis. A verification experiment was finally performed to verify the Taguchi-derived optimum processing conditions.

Table 1 Experimental parameters and corresponding levels used in this study

Experimental parameters	Corresponding levels		
	1	2	3
A: Hydrothermal time (h)	2	3	4
B: Calcination temperature (°C)	350	500	650
C: Calcination time (h)	0.5	1	2

Results and discussion

Product characteristics and reaction mechanism

Figure 2 shows the typical results of simultaneous TG–DSC analyses of the precursor. There were two stages of weight loss lying in the temperature ranges of 200–290 °C and 310–350 °C. The obvious endothermic peak centered at ~250 °C on the DSC curve was accompanied by a significant weight loss of ~25%. The abundant release of H_2O and CO_2 was detected at 250 °C by MS (see Fig. 3) and was attributed to the thermal decomposition of the precursor. As also shown in Figs. 1 and 2, the other minor exothermic reaction occurred between 300 and 350 °C, which may correspond to the oxidation of residual carbonaceous substances in the precursor as evidenced by the slight weight loss of ~2.5% along with the detected CO_2 gas.

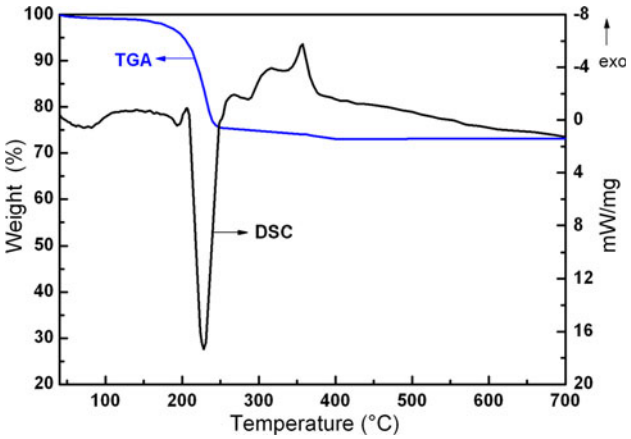

Fig. 2 Typical results of simultaneous TGA–DSC analyses of the precursor at a heating rate of 10 °C/min in static air

Table 2 Experimental results and *S/N* ratios for crystalline size and intensity ratio of UV emission to green emission (R_i) of the as-synthesized ZnO particles (Taguchi orthogonal array table of L_9 (3^4))

Exp. no.	Adopted levels (conditions)				Crystalline size (*smaller is better*)		R_i (*bigger is better*)	
	A (h)	B (°C)	C (h)	Error	Raw data (nm)	*S/N* ratio (dB)	Raw data	*S/N* ratio (dB)
1	1 (2)	1 (350)	1 (0.5)	1	15.2	−23.64	0.24	−12.40
2	1 (2)	2 (500)	2 (1)	2	23.8	−27.53	4.85	13.71
3	1 (2)	3 (650)	3 (2)	3	45.8	−33.22	1.62	4.19
4	2 (3)	1 (350)	2 (1)	3	22.6	−27.08	0.38	−8.40
5	2 (3)	2 (500)	3 (2)	1	35.7	−31.05	5.12	14.19
6	2 (3)	3 (650)	1 (0.5)	2	24.1	−27.64	1.26	2.01
7	3 (4)	1 (350)	3 (2)	2	34.3	−30.71	0.72	−2.85
8	3 (4)	2 (500)	1 (0.5)	3	18.3	−25.25	1.20	1.58
9	3 (4)	3 (650)	2 (1)	1	36.1	−31.15	3.13	9.91

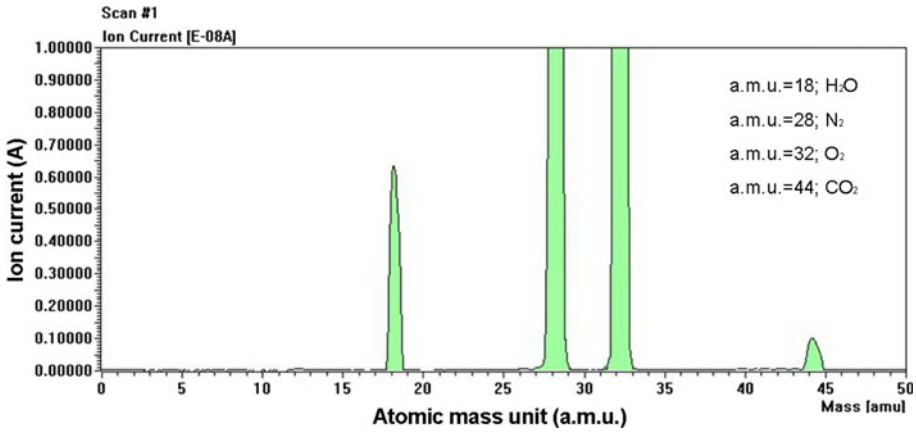

Fig. 3 MS analysis of gas escaping from the precursor when heated to 250 °C in static air

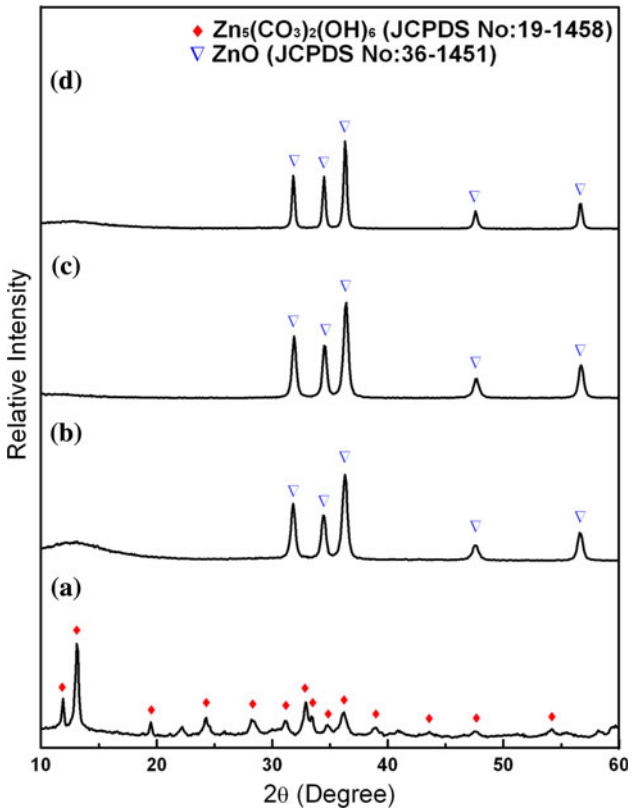

Fig. 4 XRD patterns of **a** the precursor and **b–d** the as-synthesized product calcined at **b** 350 °C for 0.5 h, **c** 500 °C for 1 h, and **d** 650 °C for 2 h

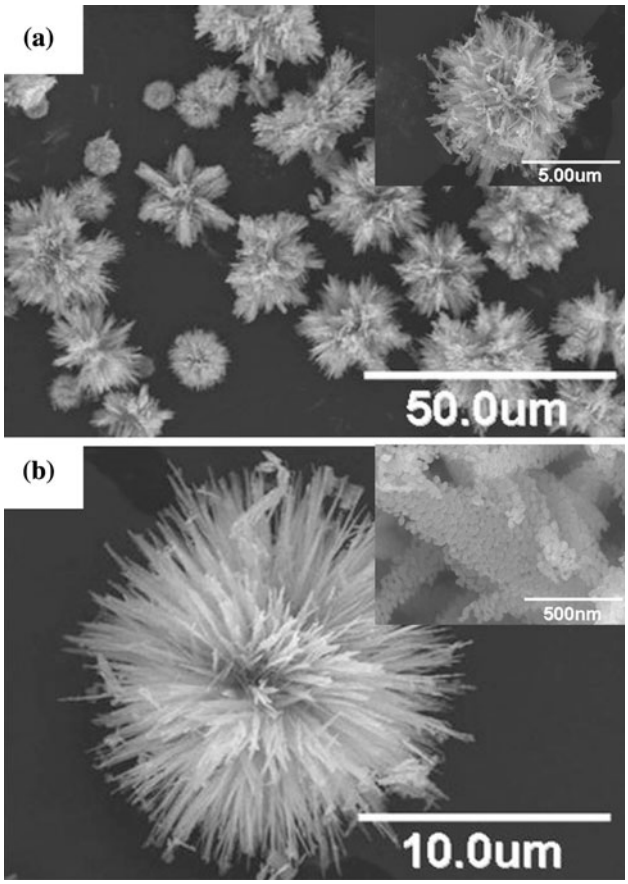

Fig. 5 SEM photographs of **a** the precursor and **b** as-synthesized product calcined at 650 °C for 2 h

Figure 4a shows the XRD pattern of the precursor precipitate, which is consistent with that of JCPDS No. 19-1458. It was thus proven that the precursor was basic zinc carbonate with the chemical composition $Zn_5(CO_3)_2(OH)_6$. After the precursors were calcined at 350 °C for 0.5 h, 500 °C for 1 h, or 650 °C for 2 h, all of the particles had the same phase composition of wurtzite ZnO with a P63mc structure (JCPDS 36-1451), and their crystalline sizes were estimated to be ~15, 25, and 46 nm, respectively (Fig. 4b–d).

Figure 5a shows that the precursor precipitate had the appearance of chrysanthemum-like particles with diameters of ~10 μm. After calcination, the shape and size of the resulting particles remained nearly the same on the microscale (Fig. 5b). This observation implied that the experimental parameters affecting the morphology of the precursor may also have an influence on that of the resulting product. The inset in Fig. 5b shows a detailed surface view of the resulting product, revealing

interconnected discrete nanocrystallites forming a loose shard. Such a feature is similar to the nanostructure of the "two-dimensional flake-like aggregates" reported by Wu et al. [9]. Based on the results of our thermal analyses and morphological observations, it is evident why Wu et al. claimed that the synthesis of flake-like single-crystal ZnO nanocrystals with porous structure can be achieved via this hydrothermal route. They also proposed that when the precursor was calcined in particle form, the dipolar ZnO nanoparticles could only rotate to a limited extent; to decrease the high surface energy, the adjacent particles self assembled and grew one by one toward the formation of large single-crystal flakes. In our opinion, however, the resulting ZnO product would inherit the prototypical shape of the precursor. We suggest that the nanostructure of so-called "two-dimensional flake-like ZnO aggregates" resulted simply from the shards of fractured precursor particles possessing a chrysanthemum-like appearance. Moreover, the nanopores among the aggregated ZnO nanocrystallites may result from the evolution of CO_2 and H_2O gases due to thermal decomposition of the precursor during heat treatment.

A possible reaction mechanism including three steps, which is consistent with the experimental results, is thus proposed as follows:

Step 1: Thermal decomposition of urea and generation of OH^- and CO_3^{2-} ions

$$NH_2CONH_2 + 4H_2O \rightarrow 2NH_4^+ + 2OH^- + CO_3^{2-} + 2H^+ \quad (2)$$

Step 2: Precipitation of basic zinc carbonate precursor under hydrothermal conditions

$$5Zn^{2+} + 6OH^- + 2CO_3^{2-} \rightarrow Zn_5(CO_3)_2(OH)_6 \downarrow \quad (3)$$

Step 3: Formation of ZnO by calcination of the precursor, i.e.

$$Zn_5(CO_3)_2(OH)_6 \rightarrow 5ZnO + 3H_2O \uparrow + 2CO_2 \uparrow \quad (4)$$

Figure 6 shows the room temperature PL spectra of the ZnO nanoparticles derived from different heat-treatment conditions. Two obvious emission peaks, a narrow near-UV emission (located at ~380 nm) and a broad green one (centered at ~500 nm), were observed in all of the PL spectra. The near-UV emission (~3.2 eV), which is close to the theoretical band gap of ZnO, comes from the recombination of free excitons [4, 9]. The green emission is the most commonly observed defect emission in ZnO nanostructures and its origin is still controversial [15]. Different hypotheses have been proposed to explain the green emission, such as transitions between the photoexcited holes and ionized oxygen vacancies (V_O^+) [16], surface defects [17], transitions between the electrons

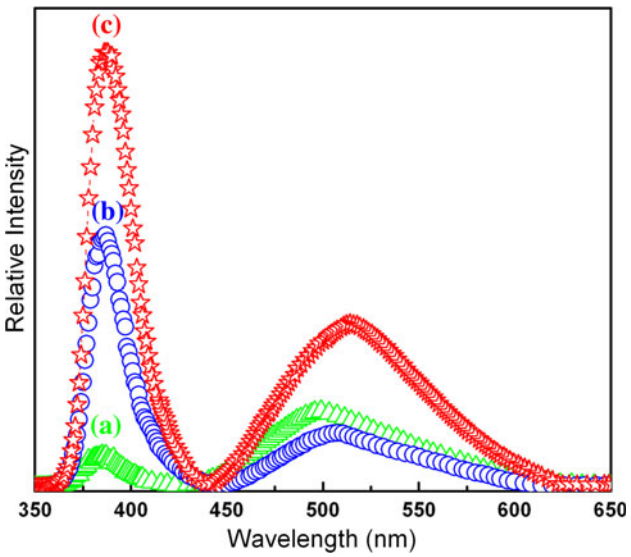

Fig. 6 Room temperature PL spectra of the nanocrystalline ZnO particles calcined under different conditions: **a** 350 °C for 0.5 h, **b** 500 °C for 1 h, **c** 650 °C for 2 h; the hydrothermal time for precursor formation was constant at 2 h

in the conduction band and deeply trapped holes at doubly ionized oxygen vacancies [18], antisite oxygen [19], and donor–acceptor transitions [20]. Considering the synthetic processes, i.e., calcination in air, it is suggested that the green emission in this study may be mainly attributed to the singly ionized oxygen vacancy, which is supported by reports of the enhancement of the green emission by annealing ZnO at temperatures above 600 °C (due to out-diffusion of O [16, 21]). Moreover, Bagnall et al. [22] demonstrated that the improvement of crystal quality (a decrease of structure defects and impurities) could result in detectable UV emission at room temperature. Therefore, the intensity ratio of the UV emission to the green emission (R_i) is a reasonable criterion to evaluate the crystalline quality of the resulting ZnO products [4, 15, 16]. The sample obtained by calcining at 350 °C for 0.5 h had the low R_i value of 0.24 (Fig. 6a). This is because a lower heat-treatment temperature, along with a shorter duration, may give rise to a larger number of defects in ZnO. The crystalline quality can be enhanced by heat-treating the samples in an O_2 atmosphere due to the effects of oxygen entering the crystal lattice, thereby improving the stoichiometric proportion of the sample and eliminating the oxygen vacancies in ZnO. This is why the sample obtained by calcining at 500 °C for 1 h had the higher R_i value of 4.85 (Fig. 6b). However, the material calcined at higher temperatures with an increase of heating time may generate a higher concentration of defects (oxygen vacancies) in the ZnO nanoparticles, likely due to the re-evaporation of oxygen. This is evident by the fact that the intensities of both the near-UV emission and the green

emission increased, but the R_i decreased ($R_i = 1.62$), as observed in the sample calcined at 650 °C for 2 h (Fig. 6c). Such phenomena may be due to the competition between oxygen atoms penetrating into the ZnO lattice and those evaporating out of the lattice in an O_2 atmosphere. At lower heating temperatures, the kinetic energy of atoms in the ZnO lattice is relatively low, and the adsorption rate of oxygen atoms is faster than the escape rate. Thus, the greater availability of oxygen atoms can compensate for the oxygen vacancies at lower temperatures (<500 °C). Conversely, the kinetic energy of atoms becomes larger at higher heating temperatures (for instance, 650 °C), likely causing an oxygen desorption rate greater than the adsorption rate, resulting in more oxygen vacancies in the ZnO lattice.

Taguchi method analysis

The Taguchi method allows the user to determine the experimental conditions having the least variability as the optimum condition. Here, the signal-to-noise (*S/N*) ratio is employed to measure the deviation of the selected quality characteristics from their desired values. The experimental conditions possessing the maximum *S/N* ratio are thus considered the optimal conditions. The *S/N* ratio is defined as [13]:

$$S/N \text{ ratio} = -10\log(\text{MSD}) \quad (\text{unit}: \text{decibel}\,(\text{dB})), \tag{5}$$

where MSD is the mean squared deviation from the target value of the output characteristic. Consistent with its application in science and engineering, the value of the *S/N* ratio is to be maximized; therefore, the value of the MSD should be minimized. Consequently, the MSD was defined differently for each of the three quality characteristics considered, namely, *bigger is better*, *smaller is better*, and *nominal is better*. In this section, the response analyses of the *S/N* ratios were used to find the optimum conditions for the synthesis of ZnO nanoparticles with smaller crystalline size and better crystalline quality (i.e., a larger R_i value). The former is the characteristic type of *smaller is better*, while the latter belongs to the *bigger is better* response. Their MSD values are, respectively, expressed as [13]:

$$\text{MSD} = \frac{1}{n}\sum_{i=1}^{n} y_i^2 \tag{6}$$

and

$$\text{MSD} = -\frac{1}{n}\sum_{i=1}^{n}\frac{1}{y_i^2} \tag{7}$$

where y_i is the result of experiment i and n is the replication number of experiments ($n = 3$ in this study).

In the above section, the experimental results show that the crystallite size and PL properties of the resulting ZnO nanoparticles could be affected by the hydrothermal time, the calcination temperature, and the calcination time. The raw data and the corresponding *S/N* ratios for the crystalline size and the R_i value of the nine designed experiments, calculated using the above equations (5)–(7), are shown in Table 2. The average *S/N* ratios for each experimental parameter at each level were summarized, and the *S/N* responses for the crystalline size and the R_i values are shown in Table 3. The *S/N* response to each parameter level is shown in Fig. 7. Here, a higher *S/N* ratio indicates a

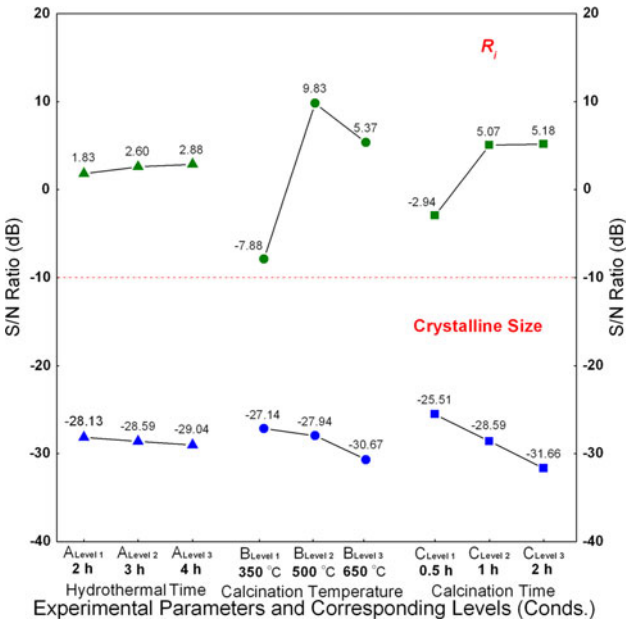

Fig. 7 Response graph of *S/N* ratios for crystalline size and R_i value

Table 3 *S/N* ratio responses for each experimental parameter at each level

Experimental parameters	Mean *S/N* ratio for crystalline size (dB)			Mean *S/N* ratio for R_i (dB)		
	Level 1	Level 2	Level 3	Level 1	Level 2	Level 3
A	−28.13	−28.59	−29.04	1.83	2.60	2.88
B	−27.14	−27.94	−30.67	−7.88	9.83	5.37
C	−25.51	−28.59	−31.66	−2.94	5.07	5.18

larger contribution by a given experimental parameter at that level to the objective function. Moreover, greater slopes of the connecting lines of the *S/N* ratios indicate larger effects of the experimental parameters on the objective function. Therefore, the optimum conditions for the crystalline size are factor A at level 1, B at level 1, and C at level 1, whereas those for the R_i value are A at level 3, B at level 2, and C at level 3. In addition, the calcination time had the most important influence on the crystalline size, while the calcination temperature had the first impact on the R_i value. However, the hydrothermal time seemed to have little effect on the crystalline size and the R_i value when compared with the other two parameters. The variation range of the *S/N* ratio with respect to the hydrothermal time was small, so it can be neglected and regarded as within experimental error. Based on our experience, however, it was found that the formation of the precursor was enhanced with an increase of hydrothermal time, resulting in an increased yield of the ZnO product. Note that the yield may be limited due to incomplete reactions and/or chemical equilibrium in the hydrothermal treatment or product loss during the washing process.

Prediction and confirmation of characteristics

To prepare ZnO products with a small crystalline size and large R_i value, the calcination temperature and time were selected as 500 °C and 1 h, respectively, as the experimental condition of 500 °C gave rise to the largest *S/N* ratio (9.83) as well as the greatest variance ($S/N_{\max} - S/N_{\min} = 9.83-(-7.88) = 17.71$) in the R_i value (see Table 3). The adoption of the other experimental condition, 1 h instead of 2 h, was a compromise to avoid overgrowth of the ZnO crystallites and to obtain an acceptable R_i value (see Fig. 7). A single-factor experiment was then carried out to investigate correlations among the hydrothermal time, product yield, crystalline size, and R_i value. As shown in Table 4, an increase of the hydrothermal time enhanced the product yield substantially. Considering processing economics, 4 h was selected as the appropriate level for the hydrothermal time; the resulting product properties remained close to the best ones (i.e., the smallest crystalline size and the largest R_i value). It is thus suggested that 4 h of hydrothermal time (A3), a calcination temperature of 500 °C (B2) and 1 h of calcination time (C2) could be the alternative optimal conditions based on the consideration of product yield. In addition, a confirmation experiment was performed and the yield and product properties are shown in Table 4.

Table 4 Product yields, crystalline sizes, and R_i values of ZnO particles synthesized with different hydrothermal times

Hydrothermal time (h)	Product yield (%)	Crystalline size[a] (nm)	R_i value
2	15	23.8	4.85
3	42	38.7	5.15
4	70	22.5	4.54

[a] The crystalline size was estimated using the Scherrer formula (see Eq. 1)

The predicted *S/N* ratio using the appropriate levels of the experimental parameters can be calculated as:

$$S/N_{\text{predicted}} = S/N_{\text{average}} + [(S/N_{\text{A3,mean}} - S/N_{\text{average}}) + (S/N_{\text{B2,mean}} - S/N_{\text{average}}) + (S/N_{\text{C3,mean}} - S/N_{\text{average}})], \quad (8)$$

where S/N_{average} is the total average *S/N* ratio, whereas $S/N_{\text{A3,mean}}$, $S/N_{\text{B2,mean}}$, and $S/N_{\text{C3,mean}}$ are the mean *S/N* ratios at the optimal level of each experimental parameter. In the case of crystalline size, the value of S/N_{average} calculated from Table 2 is (−28.59). The $S/N_{\text{A3,mean}}$, $S/N_{\text{B2,mean}}$, and $S/N_{\text{C3,mean}}$ values in Table 3 are (−29.04), (−27.94) and (−31.66), respectively. With these values, the above equation can be re-written as:

$$S/N_{\text{predicted}} = -28.59 + [(-29.04 + 28.59) + (-27.94 + 28.59) + (-31.66 + 28.59)]$$

and the predicted *S/N* ratio (−31.46) for crystalline size can thus be obtained. Then, the corresponding estimated crystalline size can be derived from Eq. (5), i.e.,

$$-31.46 = -10\log[y^2] \quad (9)$$

and the estimated crystalline size (37.41 nm) can be obtained. Both the predicted *S/N* ratio for the R_i (13.01) and the estimated R_i value (4.47) can be calculated through a similar procedure with the "*bigger is better*" analysis. Table 5 shows the comparison of the crystalline sizes and R_i values with the experimental results using the optimal conditions.

Although the crystalline size obtained from the confirmation experiment (22.5 nm) was slightly smaller than the predicted (37.41 nm) and confirmed (26.27 nm) sizes, they were all roughly consistent. According to the TEM observations (see Fig. 8), the actual crystallite size of the ZnO synthesized with the optimal conditions was estimated to be ~25 nm, which agrees with the result calculated using the Scherrer formula. As shown in Table 5, there was a good agreement between the predicted and experimental R_i values. The decrease of the *S/N* ratio from that in experiment No. 5 (14.19) to that in the confirmed experiment (13.14) was about 1.05 dB, which means that the R_i value slightly decreased. Even so, the actual R_i value of 4.54 obtained at the optimal conditions (see Table 4) was much better than those of most of the experiments shown in Table 2. Consequently, it was confirmed that the

Table 5 Comparison of the crystalline size and the R_i value with the experimental results using the optimal conditions

Condition	Crystalline size (*smaller is better*)			R_i (*bigger is better*)		
	Level	Raw data (nm)	*S/N* ratio (dB)	Level	Raw data	*S/N* ratio (dB)
Prediction	A3B2C3	37.41[a]	−31.46	A3B2C3	4.47	13.01
Confirmed prediction	A3B2C2	26.27[a]	−28.39	A3B2C2	4.42	12.90
Confirmed experiment	A3B2C2	22.5[b]	−27.04	A3B2C2	4.54	13.14

[a] The crystalline size was predicted using Eq. 9

[b] The crystalline size was estimated using Scherrer formula (see Eq. 1)

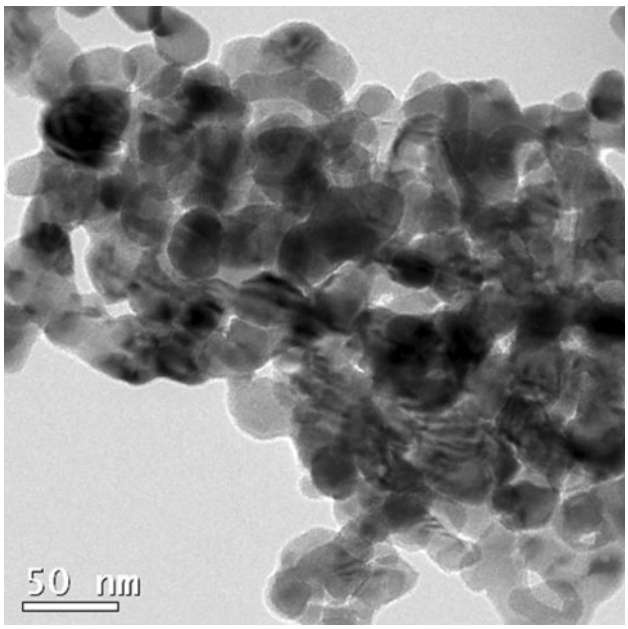

Fig. 8 TEM photograph of the ZnO nanoparticles synthesized with the optimal conditions (i.e., 4 h of hydrothermal time, a calcination temperature of 500 °C, and 1 h of calcination time)

crystalline size and R_i value (i.e., the crystalline quality) of the synthesized ZnO particles can be concurrently reduced and improved with the Taguchi method. In addition, a product yield of ~70% could be obtained under the alternative optimal conditions.

Conclusions

(1) ZnO nanoparticles were synthesized via a wet chemical route using zinc acetate dihydrate and urea as starting materials. The reaction mechanism, deduced from the XRD, TG–DSC–MS and SEM observations, was divided into three steps: first, thermal decomposition of urea and the generation of OH^- and CO_3^{2-} ions; next, precipitation of the zinc carbonate precursor under hydrothermal conditions; and finally, the formation of ZnO by calcination of the precursor. It was found that the morphology of the resulting ZnO product was similar to that of the precipitated precursor if no grinding was performed.

(2) The Taguchi method with an L_9 orthogonal array was implemented to optimize the experimental parameters for this synthesis process. The calcination time had the most influence on the crystalline size, while the calcination temperature had the greatest impact on the R_i value. The influence of the hydrothermal time, however, was insignificant compared to the other factors. Through the application of Taguchi's method, the individual optimum processing conditions for the crystalline size and the R_i value were attained.

(3) To enhance the product yield with acceptable characteristics, a set of alternative optimal conditions was proposed, i.e., a hydrothermal time of 4 h, a calcination temperature of 500 °C and 1 h of calcination time. The verification experiment revealed that ZnO nanoparticles with a small crystalline size of ~25 nm and a high R_i value of 4.54 were prepared using the processing parameters. These results were consistent with the predicted data derived from the Taguchi method. The optimized route achieved a product yield of 70% and has the advantages of a shorter production time and smaller crystalline size compared with previous reports [9, 10].

Acknowledgements The financial support of the National Science Council of the Republic of China (Taiwan) under grant number NSC 97-2221-E-606-022 is gratefully acknowledged.

References

1. Pearton SJ, Norton DP, Ip K, Heo YW, Steiner T (2005) Prog Mater Sci 50:293
2. Özgür Ü, Alivov YI, Liu C, Teke A, Reshchikov MA, Doğan S, Avrutin V, Cho SJ, Morkoç H (2005) J Appl Phys 98:041301
3. Rosina M, Ferret P, Jouneau PH, Robin IC, Levy F, Feuillet G, Lafossas M (2009) Microelectron J 40:242
4. Zhao YN, Cao MS, Li JG, Chen YJ (2006) J Mater Sci 41:2243. doi:10.1007/s10853-006-7176-5
5. Li D, Haneda H (2003) Chemosphere 51:129
6. Wang Z, Qian XF, Yin J, Zhu ZK (2004) Langmuir 20:3441
7. Zhang SC, Li XG (2003) Colloids Surf A 226:35
8. Bitenc M, Marinšek M, Crnjak Orel Z (2008) J Eur Ceram Soc 28:2915

9. Wu L, Wu Y, Lu Y (2006) Mater Res Bull 41:128
10. Kim KD, Choi DW, Choa YH, Kim HT (2008) J Mater Process Technol 202:569
11. Liu WL, Hsieh SH, Chen WJ, Lee JH (2007) Surf Coat Technol 201:9238
12. Ting JH, Chang CC, Chen SL, Lu DS, Kung CY, Huang FY (2006) Thin Solid Films 496:299
13. Roy RK (2002) Design of experiments using the Taguchi approach: 16 steps to product and process. Wiley, New York
14. Cullity BD (1978) Elements of X-ray diffraction. Addison-Wesley, Canada
15. Djurišić AB, Leung YH (2006) Small 2:944
16. Zhou J, Wang Y, Zhao F, Wang Y, Zhang Y, Yang L (2006) J Lumin 119–120:248
17. Djurišić AB, Choy WCH, Roy VAL, Leung YH, Kwong CY, Cheah KW, Gundu Rao TK, Chan WK, Lui HF, Surya C (2004) Adv Funct Mater 14:856
18. Av Dijken, Meulenkamp EA, Vanmaekelbergh D, Meijerink A (2000) J Lumin 90:123
19. Lin B, Fu Z, Jia Y (2001) Appl Phys Lett 79:943
20. Reynolds DC, Look DC, Jogai B (2001) J Appl Phys 89:6189
21. Meng XQ, Shen DZ, Zhang JY, Zhao DX, Lu YM, Dong L, Zhang ZZ, Liu YC, Fan XW (2005) Solid State Commun 135:179
22. Bagnall DM, Chen YF, Shen MY, Zhu Z, Goto T, Yao T (1998) J Cryst Growth 184(185):605